

Searches for the Anomalous FCNC Top-Higgs Couplings at the LHeC

Hao Sun* and XiaoJuan Wang

Institute of Theoretical Physics, School of Physics & Optoelectronic Technology,
Dalian University of Technology, No.2 Linggong Road, Dalian, Liaoning, 116024, P.R.China

Abstract

We perform an updated analysis on searches for the anomalous flavor changing neutral current(FCNC) Yukawa interactions between the top quark, the Higgs boson, and either an up or charm quark(tq , $q = u, c$). We probe the observability of the FCNC top-Higgs couplings through the process $e^-p \rightarrow \nu_e \bar{t} \rightarrow \nu_e h \bar{q}$ at the Large Hadron Electron Collider(LHeC) where the Higgs boson decays to a $b\bar{b}$ pair. We compare the results from both the Cut-based method and the Multivariate Analysis(MVA) based method. The impact of light, charm jet mis-identification rates and B-tagging efficiencies on the discovery potential are quantified. Our results show that, at a 7 TeV LHeC with a 60 GeV electron beam and 1000 fb^{-1} integrated luminosity, the expected limit on $\text{Br}(t \rightarrow uh)$ can be probed down to $0.113(0.093)\%$ with the Cut-based(MVA based) analysis at the 95% confidence level. At a 50 TeV high energy LHeC, the corresponding limit can be probed down to $0.03(0.022)\%$.

Keywords: Top quark, Higgs boson, Anomalous Couplings, LHeC

PACS numbers: 14.65.Ha, 12.60.-i

*Corresponding author: haosun@mail.ustc.edu.cn haosun@dlut.edu.cn

1 INTRODUCTION

The discovery of the Higgs boson at the Large Hadron Collider(LHC)[1][2] is a major step towards understanding the electroweak symmetry breaking(EWSB) mechanism and marks a new era in particle physics. The precise measurement of the Higgs boson and the top quark properties would provide the possibility of searching for the anomalous flavor changing neutral current(FCNC) Yukawa interactions between them and either an up or charm quark(tqh, $q = u, c$). According to the Standard Model(SM), FCNC processes are forbidden at tree level and very much suppressed at higher orders due to the Glashow-Iliopoulos-Maiani(GIM) mechanism[3]. For instance, the $t \rightarrow qh$ ($q = u, c$) branching ratio is of the order of $\sim 10^{-10}$ or even below. In models beyond the SM(BSM), the GIM suppression can be relaxed, yielding effective tqh couplings orders of magnitude much larger than those of the SM and therefore being detectable using current experimental data. Observations of such anomalous top-Higgs couplings would provide a clear signal of new physics. Examples of such model extensions[4] are, for instance, the Minimal Supersymmetric Model(MSSM) with/without R-parity Violating [5][6][7][8][9][10][11][12][13][14][15][16][17][18][19], the two Higgs Doublet Model(2HDM) [20][21][22][23][24][25][26][27][28][29][30][31], the Warped Extra Dimensions Model [32][33], the Alternative Left-Right symmetric Model(ALRM)[34], the Little Higgs with T parity Model(LHT)[35], the Quark Singlet model(QS)[36][37][38], etc.

Considering the FCNC Yukawa interactions in the effective field theory(EFT) framework, the SM Lagrangian can be extended simply by allowing the following terms,

$$\mathcal{L} = \kappa_{tuh} \bar{t}uh + \kappa_{tch} \bar{t}ch + \text{h.c.}, \quad (1)$$

where κ_{tuh} and κ_{tch} are the real parameters and denote the flavor changing couplings of Higgs to up-type quarks. Now we have m_t minus m_h larger than m_c , m_u and m_b . In addition to the usual decay mode $t \rightarrow w^\pm b$, the top quark can also decay into a charm or up quark associated with a Higgs boson. Similarly, the new tqh interactions can also affect the width of the Higgs boson, through its additional decay into an off-shell top that subsequently leads to a single w , namely $h \rightarrow u(c)(t^* \rightarrow wb)$ where t^* denotes off-shell

top quark. Therefore, the total decay width of the top quark(Γ_t) and Higgs boson(Γ_h) are

$$\begin{aligned}\Gamma_t &= \Gamma_{t \rightarrow w^- b}^{\text{SM}} + \Gamma_{t \rightarrow ch} + \Gamma_{t \rightarrow uh} \\ \Gamma_h &= \Gamma_h^{\text{SM}} + \Gamma_{h \rightarrow u(\bar{t}^* \rightarrow \bar{b} w^-)} + \Gamma_{h \rightarrow \bar{u}(t^* \rightarrow b w^+)} + \Gamma_{h \rightarrow c(\bar{t}^* \rightarrow \bar{b} w^-)} + \Gamma_{h \rightarrow \bar{c}(t^* \rightarrow b w^+)}.\end{aligned}\quad (2)$$

$\Gamma_{t \rightarrow w^- b}^{\text{SM}}$ is the normal top decay width in the SM. Its analytical formula up to next-to-leading order(NLO) can be found in Ref.[39]. The $t \rightarrow u(c)h$ partial decay width is given as[40]

$$\Gamma_{t \rightarrow u(c)h} = \frac{\kappa_{tu(c)h}^2}{16\pi} m_t [(\tau_{u(c)} + 1)^2 - \tau_h^2] \sqrt{1 - (\tau_h - \tau_{u(c)})^2} \sqrt{1 - (\tau_h + \tau_{u(c)})^2} \quad (3)$$

where $\tau_h = \frac{m_h}{m_t}$, $\tau_{u(c)} = \frac{m_{u(c)}}{m_t}$. Γ_h^{SM} is the normal two body Higgs decay width in the SM. The other terms related to the Higgs boson three-body decays are numerically estimated. The branching ratio for $t \rightarrow qh$ is then given by

$$\text{Br}(t \rightarrow u(c)h) = \frac{\kappa_{tu(c)h}^2}{\sqrt{2} G_F m_t^2} \frac{(1 - \tau_h^2)^2}{(1 - \tau_w^2)^2 (1 + 2\tau_w^2)} \quad (4)$$

where $\tau_w = \frac{m_w}{m_t}$ and G_F is the fermi constant. With parameters that would present in the following we get $\text{Br}(t \rightarrow u(c)h) \approx 0.512 \kappa_{tu(c)h}^2$ which is used in the extraction of the couplings in our analysis. Since the analysis does not distinguish between the $t \rightarrow ch$ and $t \rightarrow uh$ final states which have similar acceptances, we use $t \rightarrow uh$ mode as reference throughout this work without other statement.

The searches for the anomalous FCNC top-Higgs coupling have been investigated at the LHC and the direct limits on the branching ratio are set from the collider experiments. The most stringent constraint through direct measurements was reported by the CMS collaboration from a combination of the multilepton channel and the diphoton plus lepton channel[41]. The results are corresponding to 19.5 fb^{-1} data at the center-of-mass energy of 8 TeV. The 95% confidence level(C.L.) upper limit on $\text{Br}(t \rightarrow u(c)h)$ has found to be $4.5(5.6) \times 10^{-3}$ for a Higgs boson mass of 126 GeV. Similarly, the ATLAS collaboration has performed the search through $t \rightarrow qh$ decay followed by $h \rightarrow \gamma\gamma$ in a data set of proton-proton collisions, consisting of 4.7 fb^{-1} at $\sqrt{s} = 7 \text{ TeV}$ and 20.3 fb^{-1} at $\sqrt{s} = 8 \text{ TeV}$ [42][43].

An upper limit is set on the $t \rightarrow qh$ branching ratio of 0.79% at the 95% confidence level. Except for the direct collider measurements, low energy measurements in flavor mixing processes can also be used to provide indirect constraints on the anomalous tqh vertex. At one-loop level, the $D^0 - \bar{D}^0$ mixing observable can receive sizeable contributions with such an unvanishing flavor violating tqh coupling[44]. Use data observed on $D^0 - \bar{D}^0$ mixing, the upper limit of $\text{Br}(t \rightarrow qh) < 5 \times 10^{-3}$ can be obtained.

Studying the FCNC top-Higgs interactions is therefore important from a theoretical perspective. Many phenomenological studies are performed based on the experimental data, through a widely studied $t \rightarrow qh$ decays and a single top Higgs associated production mode. For instance, Ref.[45] performed a study on the top-Higgs couplings through several productions and found that the process $pp \rightarrow t\bar{t}h(\bar{t}jh) \rightarrow b\ell\nu jjj$ can be extremely useful in providing strong bounds on the tqh couplings of the order of 1.7×10^{-3} with 2σ sensitivities using the full data at $\sqrt{s} = 8$ TeV LHC. And this sensitivities can be improved just a bit more to 1.1×10^{-3} for the 14 TeV LHC with 300 fb^{-1} data. The similar study was performed in Ref.[46] through $pp \rightarrow tjh \rightarrow b\ell\nu j\gamma\gamma$, giving the upper limits of $\text{Br}(t \rightarrow uh) < 0.23\%$ and $\text{Br}(t \rightarrow ch) < 0.26\%$ with an integrated luminosity of 3000 fb^{-1} at 3σ sensitivity at the 14 TeV LHC. Ref.[47] quoted a 95% C.L. limit from the $pp \rightarrow tt \rightarrow Wb + hq \rightarrow \ell\nu b + \ell\ell q$ final state. The sensitivities of $\text{Br}(t \rightarrow qh) < 5(2) \times 10^{-4}$ were estimated with an integrated luminosity of $300(3000) \text{ fb}^{-1}$ at $\sqrt{s} = 14$ TeV. And Ref.[48] estimated the sensitivity based on 100 fb^{-1} of 13 TeV data. There the branching ratio $\text{Br}(t \rightarrow u(c)h)$ were obtained to be 0.22(0.33)%, 0.15(0.19)% and 0.36(0.48)% from multilepton searches, vector boson plus Higgs search and fully hadronic search respectively. More, Ref.[49] derived model-independent constraints on the tqh couplings that arise from the bounds on hadronic electric dipole moments. Ref.[50] studied the NLO QCD effects in the anomalous $t \rightarrow qh$ decay. The NLO QCD effects of top Higgs associated production with FCNC couplings were considered in Ref.[51]. Many other related studies include, for example, Ref.[52][53][54][55][56], etc, and references there in.

In our present paper, we perform an updated study on the anomalous FCNC Yukawa

interactions between the top quark, the Higgs boson, and either an up or charm quark(tqh , $q=u,c$) at the Large Hadron Electron Collider(LHeC). A former study was performed in Ref.[57]. There we briefly reviewed the search of this anomalous couplings at the LHeC at a very basic level. A comparison between the different charge current(CC) and neutral current(NC) production channels were provided. There comes the conclusion that the CC induced $e^-p \rightarrow \nu_e \bar{t} \rightarrow \nu_e h \bar{q}$ production with $\gamma\gamma$, $b\bar{b}$ pair and $\tau^+\tau^-$ decays are the favored candidate channels. $h \rightarrow \gamma\gamma$ channel was chosen because of its demonstrated high importance for inclusive Higgs boson studies, with a rather clean signature at the normal LHC. However, for a Higgs boson mass around 125 GeV, $e^-p \rightarrow \nu_e \bar{t} \rightarrow \nu_e h \bar{q}$ production with $h \rightarrow \gamma\gamma$ decay at the LHeC, suffers from its small branching ratio(0.23%), thus is not the most favored one. For $h \rightarrow \tau^+\tau^-$ channel, since the τ event reconstruction is challenge, thus making this decay channel less favored. In this paper we choose the $h \rightarrow b\bar{b}$ mode which is more interesting than the other channels. In addition, the impact of light, charm jet mis-identification rates and B-tagging efficiencies on the discovery potential are quantified in our following discussions. Discovery potential for the 50 TeV high proton energy beam is also considered.

Our paper is organized as follows: Section 2 is arranged to present the analysis and numerical results in detail. There comes the subsections include signal and background analysis, simulation and the LHeC discovery potential. Typically, we perform our analysis in a Cut-based method and a Multivariate Analysis(MVA) based method. A comparison on their impact on the FCNC coupling discovery potential is performed. The expected limits are then obtained based on a event number counting method. Finally we summarize our conclusion in the last section.

2 PROCESS ANALYSIS AND NUMERICAL CALCULATIONS

2.1 Signal and Background Analysis

The considered signal productions with top-Higgs FCNC couplings can be written as

$$e^-p \rightarrow \nu_e \bar{t} \rightarrow \nu_e h \bar{q} \rightarrow \nu_e b \bar{b} \bar{q}, \quad (5)$$

where $q=u,c$. The Feynman diagram is plotted in Fig.1 for the partonic process $e^- \bar{b} \rightarrow \nu_e \bar{t} \rightarrow \nu_e h \bar{q} \rightarrow \nu_e b \bar{b} \bar{q}$. This production belongs to the charge current production[57] at the LHeC. As can be seen, the studied topology of our signal gives rise to the \cancel{E}_T + jets signature characterized by three(or more than three) jets and a missing transverse momentum(\cancel{E}_T) from the undetected neutrino. Two of the jets should be tagged as B-jets. The combination of the two B-jets should appear as a narrow resonance centered around the SM Higgs boson mass. Together with the remaining light jet(s), they should be able to reconstruct a resonant top quark.

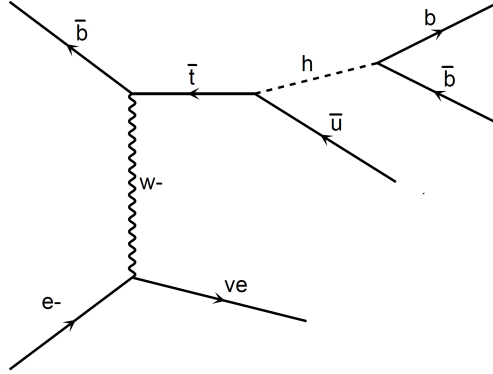


Figure 1: Feynman diagram for the partonic process $e^- \bar{b} \rightarrow \nu_e \bar{t} \rightarrow \nu_e h \bar{q} \rightarrow \nu_e b \bar{b} \bar{q}$ at the LHeC through flavor changing top-Higgs interactions.

The main backgrounds come from both the reducible and irreducible ones. The crucial irreducible backgrounds which yield exactly the same final states to the signal are listed

bellow. See,

$$e^-p \rightarrow \nu_e(h \rightarrow b\bar{b})j \quad (6)$$

$$e^-p \rightarrow \nu_e(z \rightarrow b\bar{b})j \quad (7)$$

which contain three QED couplings, are noted as “bakh” and “bakz” respectively,

$$e^-p \rightarrow \nu_e(g \rightarrow b\bar{b})j \quad (8)$$

which contains two QED couplings and two QCD couplings, is noted as “bakg”. Notice here and bellow, $j = g, u, \bar{u}, d, \bar{d}, c, \bar{c}, s, \bar{s}$. One source of the most important potentially reducible backgrounds is

$$\begin{aligned} e^-p &\rightarrow \nu_e jjj \\ e^-p &\rightarrow \nu_e jjb/\bar{b} \end{aligned} \quad (9)$$

due to a mis-identification of one or more of the final state light jets to B-jets. These processes contain two QED couplings and two QCD couplings as well. We refer them as “bakvej” (include the “bakg” background). Another source of reducible background is single top production. As can be seen, the signal process studied in our paper is essentially single top production at the e^-p collider, followed by a particular decay chain. This means that SM single top production and decay is an important background to our signal production under consideration. We refer these backgrounds as “bakt”. Among them, production of

$$e^-p \rightarrow \nu_e(\bar{t} \rightarrow (w^- \rightarrow jj)\bar{b}) \quad (10)$$

is one example. The produced top quark will decay to a w boson and a B-jet. The hadronic decay of the w boson to non-B-jets final states, which might mis-tagged as a B-jet, make this production a dangerous background. We also consider some neutral current (NC) production backgrounds:

$$\begin{aligned} e^-p &\rightarrow e^- jjj \\ e^-p &\rightarrow e^- jjb/\bar{b} \\ e^-p &\rightarrow e^-(g \rightarrow b\bar{b})j. \end{aligned} \quad (11)$$

These are NC multi-jet backgrounds and belong to reducible ones. We use “bkgej” as a simple notation to refer them. Finally, we include some Feynman diagrams for the most important backgrounds in Fig.2. Typically, Fig.2 (a),(b),(c),(d, e),(f) and (g, h, i) correspond to bakh, bakz, bakg, bakvej, bakt and bakej respectively.

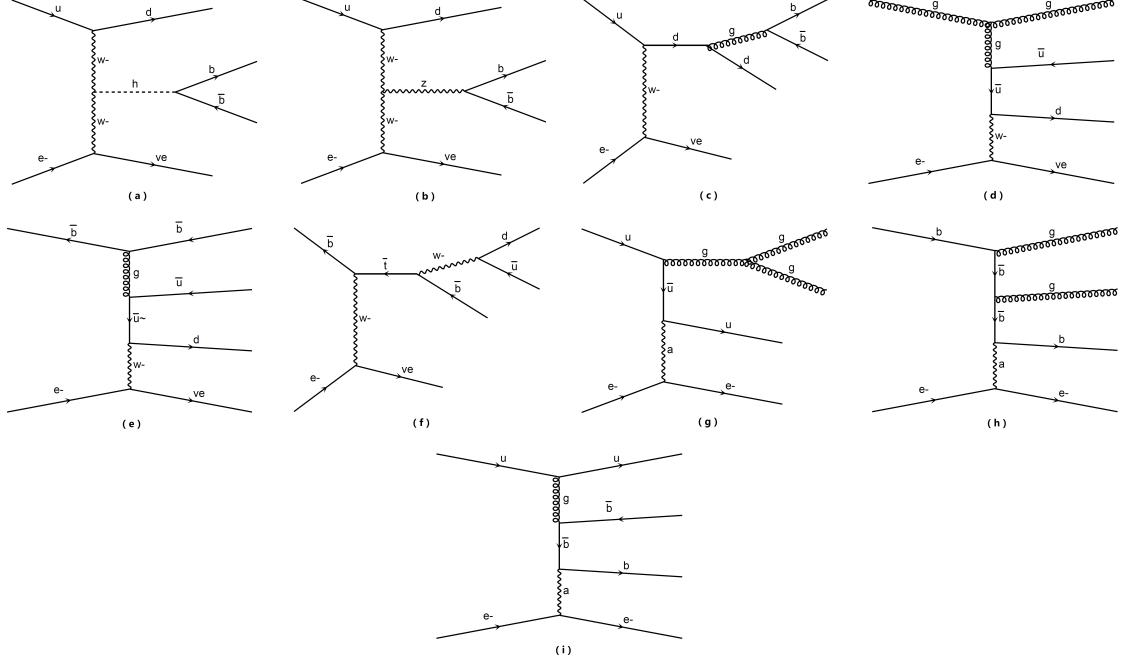


Figure 2: Example of partonic Feynman diagrams for the reducible and irreducible backgrounds correspond to the signal.

2.2 Simulation

For the collider phenomenology, we use FeynRules[58] to extract the Feynman Rules from the Lagrangian in Eq.(1). The model is generated into Universal FeynRules Output(UFO) files[59] and then fed to the Monte Carlo event generator MadGraph@NLO[60] for the generation of event samples. We pass the generated parton level events on to PYTHIA6.4[61] which handles the initial and final state parton shower, hadronization, heavy hadron decays, etc. When generating the parton level events, we set the renormalization and factorization scale at Z-boson mass. We set CTEQ6L[62] parton distribution

function, with α_s (the strong coupling constant) evaluated consistently at all stages (PDFs, hard scattering and decays). We take all the low flavored quarks, gluon and also the b-quark fluxes inside proton. We use FASTJET[63] for jet clustering instead of using the PYCELL routine in PYTHIA6.4. Jets are anti-kt clustered[64] with a cone of radius $\Delta R(j) = \sqrt{\Delta\eta^2 + \Delta\phi^2} = 0.7$. We do not include any matching algorithm used to interface MadGraph with Pythia. One can reproduce our sample with default parameters set in Pythia, except a special tune on MSTP(11). Considering our signal and background processes, we also apply B-jet tagging technique in our analysis. Final tagged B-jets are mainly resulted from three sources. One source is a jet that matches a B-flavored hadron and tagged to be a B-jet. The default B-jet tagging rate is taken to be $\epsilon_b = 60\%$ without other statements. The second source is a jet that matches a C-flavored hadron and mis-tagged to be a B-jet. We accept it as a B-jet only if it is mis-tagged with probability $\epsilon_c = 0.1$. And the third is a light jet mis-tagged as a B-jet where we assume the mis-tagged rate to be $\epsilon_{\text{light}} = 0.01$. The top quark, z boson and w boson are allowed to be decayed freely. The input heavy particle masses are taken as $m_t = 173.2$ GeV, $m_z = 91.1876$ GeV, $m_w = 79.82$ GeV and $m_h = 125.7$ GeV, respectively. For the LHeC colliding energy, we concentrate on the 7 TeV proton beam at the LHC as well as the 50 TeV proton beam at the future FCC-HE[65] and an energetic new electron beam with the energies of 60 GeV which consistent with the default design energy of the LHeC project[66].

To estimate the event rate at parton level for the signal, we apply the following basic pre-selections:

$$\begin{aligned}
\cancel{E}_T^{\text{missing}} &\geq 15 \text{ GeV}, \\
p_T^{k_0} &\geq 15 \text{ GeV}, \quad k_0 = j, b, \ell, \\
|\eta^j| &< 5, |\eta^b| < 5, |\eta^\ell| \leq 3, \\
\Delta R(k_1 k_2) &> 0.4, \quad k_1 k_2 = jj, j\ell, jb, bb, b\ell.
\end{aligned} \tag{12}$$

where $\Delta R = \sqrt{\Delta\Phi^2 + \Delta\eta^2}$ is the separation in the rapidity-azimuth plane, $p_T^{\text{jet}, b, \ell}$ are the transverse momentum of jets, B-jets and leptons, $\cancel{E}_T^{\text{missing}}$ is the missing transverse momentum. The cuts are defined in the lab frame. We stress that the cuts in Eq.(12) are

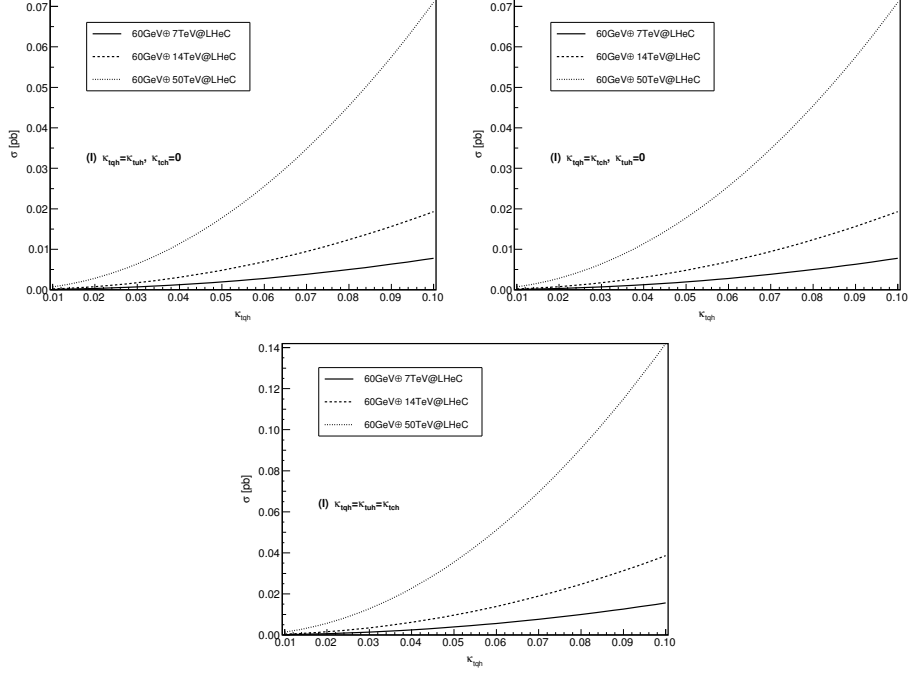


Figure 3: The signal cross sections for $e^-p \rightarrow \nu_e \bar{t} \rightarrow \nu_e h \bar{q} \rightarrow \nu_e b \bar{b} \bar{q}$ as a function of the top-Higgs FCNC couplings κ_{tqh} at the 7, 14 and 50 TeV LHeC.

the very basic ones and might be changed later in our following discussion. In order to obtain the anomalous FCNC tqh coupling effects, we need to simulate the signal contributions precisely together with all the backgrounds. We use the same pre-selections for the backgrounds as well as the identical conventions and parameter sets as pre-described. In Fig.3, we show the dependence of the cross sections σ as a function of the top-Higgs FCNC couplings κ_{tqh} at the 7TeV, 14TeV and 50 TeV LHeC for three different cases:

- (I) $\kappa_{tqh} = \kappa_{tuh}, \kappa_{tch} = 0$
- (II) $\kappa_{tqh} = \kappa_{tch}, \kappa_{tuh} = 0$
- (III) $\kappa_{tqh} = \kappa_{tuh} = \kappa_{tch}$.

The cross section of 50 TeV can be 14 times larger than that of 7 TeV. As we said above, the analysis does not distinguish between the $t \rightarrow ch$ and $t \rightarrow uh$ final states, we use $t \rightarrow uh$ mode through our analysis. The total cross section for these reactions thus can

be split into three contributions

$$\sigma = a_0 + a_1 \kappa_{\text{tuh}} + a_2 \kappa_{\text{tuh}}^2 \quad (13)$$

where a_0 is the SM prediction, the term a_1 linear in κ_{tuh} arises from the interference between SM and the anomalous amplitudes, whereas the quadratic term a_2 is the self-interference of the anomalous amplitudes.

2.3 Event Selection and Resonance Reconstruction

Now we turn to discuss event selections step by step in more details. We define the notation of “cut1” first: cut1 stands for the basic generator level cuts in Eq.(12). The cross sections for the signal and backgrounds after our Monte Carlo simulation, with cut1, are about 5.8(52.8) fb for the signal with $\kappa_{\text{tuh}} = 0.1$, 1.5(14.0) pb for the single top background(bakt), 50.5(244.6) pb for the NC multi-jet QCD background(bakej), 11.2(50.2) pb for the CC multi-jet QCD background(bakvej), 63.1(234.1) fb for the associated Higgs jet background(bakh) and 71.1(297.5) fb for the associated z jet background(bakz), respectively. For the same reason of simplicity, we name the signal production as “signal0.1”. Results are listed in the first column in Table.1(Table.2) for the 7TeV(50 TeV) LHeC. We see here the NC multi-jet QCD production, with the cross section of 50.5(244.6) pb, is the most largest one at this stage.

We define the notation of “cut2” here: cut2 means a selection that includes the following three conditions:

$$e^- p \rightarrow \cancel{E}_T^{\text{missing}} + 0 \ell + \geq 3 \text{ jets, (with at least 2 tagged B-jets).} \quad (14)$$

First, a no-lepton selection is imposed to make sure that the passed events do not contain triggered lepton(s) in the final state. This condition helps to reject NC multi-jet QCD background efficiently. Secondly, we require the selected events must contain at least three jets. The distribution of the number of jets(N_{jet}) is shown in the left panel of Fig.4 for 7(50) TeV. All distributions for the signal and different backgrounds are unit normalized and plotted separately. The red area relates to the signal while the colour lines correspond

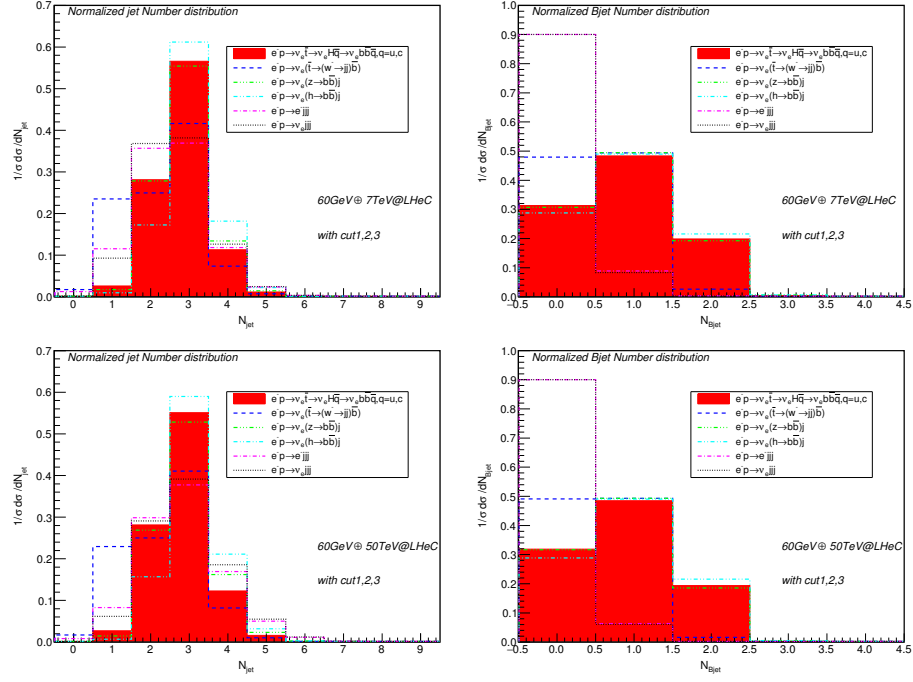


Figure 4: The distribution of the number of jets(N_{jet}) in the left panel and the distribution of the number of tagged B-jets(N_{Bjet}) in the right panel for the signal and the SM backgrounds. Here the B-tagging efficiency is $\epsilon_b = 0.6$. The light, charm jets misidentification rates are $\epsilon_c = 0.1$ and $\epsilon_{\text{light}} = 0.01$. All the distributions are normalized.

to the backgrounds. We see the events that contain three jets account for around 50% to the total, for both the signal and the backgrounds. More than 60% events are kept when we include events with more than three jets. Thirdly, we require that there must be at least two jets are tagged to be B-jets. The distribution of the number of the tagged B-jets(N_{Bjet}) is shown in the right panel of Fig4. Notice the B-tagging is performed at a 60% efficiency working point. The mis-tagging rate for the low flavor jets are all taken into accounts. The normalized distribution does not distinguish with each other very much between 7 and 50 TeV. It is clear that the selection of at least two B-jets could reduce all the backgrounds, especially multi-jet QCD backgrounds(purple dash-dotted line and black dotted line) and bakt(blue dashed line) backgrounds efficiently. By imposing cut2, the most critical selection, all the backgrounds are reduced obviously. More details can be seen in the third column in Table.1 and Table.2.

A $\cancel{E}_T^{\text{missing}} > 20$ GeV cut is defined to be “cut3”. This cut can again result in strong reduction in the NC $e^-p \rightarrow e^-jjj$ background. But it is not quite efficient to the other productions, and has little impact on the signal as well. After imposing these three cuts, we see the bakej background drops from 50.5(244.6) pb to 0.89(7.39) fb for 7(50) TeV, and leads to the largest reject efficiency. The bakvej background drops from 11.2(50.2) pb to 20.3(117.2) fb with the reject efficiency of more than 99%. The bakh and bakz backgrounds are not very far from each other, about 10(40) fb after the three selections. They are rejected with a efficiency of around 85%. The bakt background drops from 1.5(14) pb to 27.2(258.7) fb, with a reject efficiency of 98%. Finally, we can find that the signal events are selected with a selection efficiency of order 13% for both 7 and 50 TeV. Details can be found in the first four columns.

Although the selections and rejections are quite efficient, the backgrounds are still much larger than the signal. Our next step is to reconstruct the resonance in the selected events, typically, the reconstruction of the Higgs boson and the top quark. As can be seen, the Higgs boson can be easily reconstructed by considering the two tagged B-jets in the final state and summing over their 4-momentum. If more than two B-jets appear, we reconstruct the Higgs by checking which two can reconstruct the mass closer to the input

Higgs mass. Well, events with more than two B-jets rarely happen in our case, as can be seen in the distribution of N_{Bjet} in Fig.4[right panel]. The reconstructed Higgs mass is presented in Fig.5[first two panels], Again, the signal is present in the red zone. We display different backgrounds separately and each of them is unit normalized. The bckj backgrounds are already quite small after cut3, thus not shown in the figures here and following. We find that the reconstructed Higgs mass for the signal is peaked strongly at ~ 115 GeV, however, 10 GeV lower than the real input mass ~ 125 GeV. This is not strange. Indeed, the peak is always shown up to the left side of the actual mass due to jet energy smearing. And the magnitude of shift depends on the jet-cone size which, in our case, is chosen to be 0.7. A lower jet-cone size, for example, 0.5, can lead to a little more “left side” shift of our reconstructed Higgs mass. And there is no energy scale correction applied, thus the Higgs mass is lower than 125 GeV. This is also true for the top quark as well as the $z(w)$ boson mass reconstructions for the backgrounds. For instance, as shown in Fig.5[first two panels], the green dash-dot-dotted line, correspond to the bakz background. A z boson is reconstructed with the mass close to but less than $m_z = 91.1876$ GeV.

In Fig.5[second two panels], we present the mass reconstruction of the top quark. See the red zone for the signal. The top quark is finally reconstructed by taking the reconstructed Higgs and the remaining light jets as its constituents. More than one other jets can appear in the final selected events. We choose the jets that can reconstruct the mass closest to the top mass, say, the jets that make the Higgs jets system(m_{hj}), closest to $m_t = 173.2$ GeV. All the other backgrounds are not strongly peaked around the top mass, thus make them well separate, except the bakt background (blue dashed line). For bakt we recall the most important contribution is the reaction $e^-p \rightarrow \nu_e(\bar{t} \rightarrow (w^- \rightarrow jj)\bar{b})$. One anti-b quark is originated from the top quark while the other one is from the mis-tagging of the hadronic w decay. From here we see that a promising avenue to reduce the single top background is to improve B-tagging efficiencies and to reduce the light(charm) jet

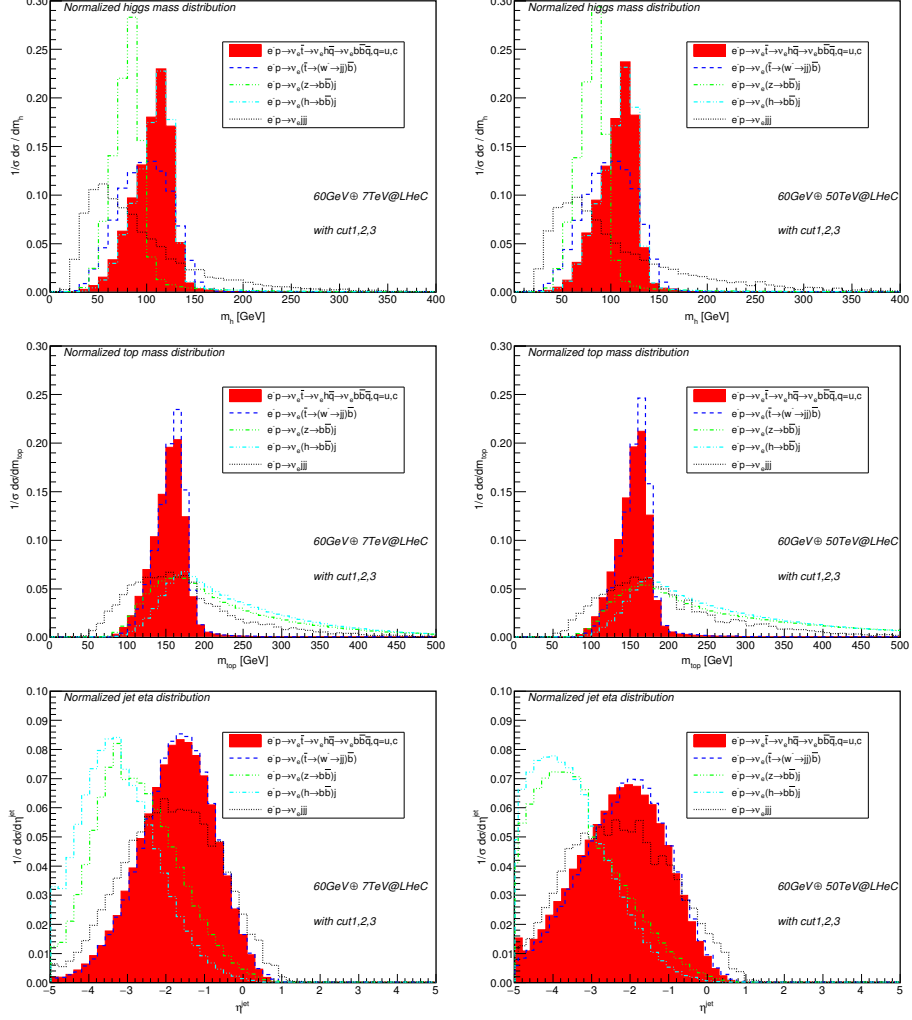


Figure 5: Higgs mass, top quark reconstruction and forward light jet rapidity distribution for the signal($\kappa = 0.1$) compares to the SM backgrounds. Here the B-tagging efficiency is $\epsilon_b = 0.6$. The light, charm jets mis-identification rates are $\epsilon_c = 0.1$ and $\epsilon_{\text{light}} = 0.01$. All the distributions are normalized.

mis-identification rates. A more detailed study of the dependence on them will appear in the following.

2.4 LHeC Discovery Potential

We will aim at finding the most efficient selections in order to allow the best separation between noise-related and signal-related events and show the search strategies for the anomalous tqh couplings. This requirement is satisfied when the signal significance is maximized. We adopt two different methods in our analysis:

- Cut-based analysis: in this method, we simply apply different cuts on various kinematic variables in order to optimize the signal significance.
- Multivariate analysis: in this method, we employ multivariate techniques, use several different input variables, to give better signal to background discrimination, thus resulting better signal significance.

Here the signal significance is defined by

$$\mathcal{SS} = \frac{S}{\sqrt{S+B}}. \quad (15)$$

We define the signal to background ratio by

$$\mathcal{R} = \frac{S}{B} \quad (16)$$

and their purity by

$$\mathcal{P} = \frac{S}{S+B}. \quad (17)$$

Here S and B relate to the numbers of the signal and background events respectively, under expected luminosity. These definitions are used in Tables.1 and 2.

2.4.1 Optimized selections and Cut-based method Analysis

Here we first study the Cut-based method. After applying the above pre-selections (cut1, cut2 and cut3) and adopting the resonant reconstructions, the choice of further selections

thus become straightforward. Following information in Fig.5, we require the invariant mass of the reconstructed top to be in the range $m_t \in [148 \text{ GeV}, 178 \text{ GeV}]$. We define this cut to be “cut4”. It reduces the bakz, bakh, bakej and bakvej backgrounds obviously, which do not contain a reconstructed top quark. The reject efficiencies are 82.1(85.9)%, 82.2(85.2)%, 73(77.5)% and 80.7(81.2)% for 7TeV(50TeV), respectively. Notice unless mentioned otherwise, all the efficiencies are quoted with respect to the previous selection. For the signal and the bakt background which contain a reconstructed top quark, about half of the events pass the selection, lead to a 54.5(40.2)% and 54.8(39)% select(reject) efficiency for them at 7 and 50 TeV respectively. Now the cross sections of the other backgrounds turn to the same order compare to the signal. The most largest background is the single top background which is 16.3(157.7) fb. more than 40 times larger than the signal. To reduce it, we require the events should not pass the selection if the B-j system belongs to $[50\text{GeV}, 90\text{GeV}]$. This selection is defined to be “cut5”. With this requirement, the bakt background is reduced to 0.84(7.37) fb, same order of the signal now. We also impose “cut6”: two B-jets invariant mass should out of the z boson mass window, which can reduce, for example, the bakz background. In addition, once a Higgs boson has been identified, its mass is required to lie within a fixed window around 115 GeV. Specifically we require the condition to be $100 \text{ GeV} < m_h < 130 \text{ GeV}$. Cross sections after imposing all these cuts are presented in columns 5-7 in Table.1 and Table.2.

Once all the above selections are met, the next question is whether there are more choices of cuts that can be used to improve the signal significance. Consider of signal and backgrounds, a forward jet cut is worth being considered. The forward jet lies very close to the direction of the incoming proton, i.e., like the z, Higgs production via the vector boson fusion(VBF) through the normal proton proton collision at the LHC. In contrast to VBF, instead of a jet with large rapidity gap with the forward jet, in our productions, we have the neutrino. The more massive the heavy particle is, the energy of the forward jet is becoming less, so it lies more close to the proton direction, i.e., larger rapidity. This is, however, a good characteristics if our signal is the SM Higgs production as discussed in Ref.[67] or heavy Higgs production as discussed in Ref.[68]. Please recall

that in our case the SM Higgs production is one of the backgrounds. We thus expect the candidate light jets to be centrally produced. This selection cut(defined as “cut8”) which is used to reduce the large rapidity light jets is called the forward jet veto. We introduce $|\eta^j| < 2.5(3)$ for 7(50)TeV. It has severe impact on the processes of, i.e., SM Higgs jet associated production and z jet associated production, in the forward rapidity region. The distribution of the forward jet rapidity is displayed in Fig.5[The third two panels]. We see the bakz and bakh backgrounds enhance at the range $|\eta^j| > 2.5$ and $|\eta^j| > 3$ for 7 TeV and 50 TeV respectively. The forward jet veto cut can reduce bakz(bakh) to 0.017(0.09) fb at the 7TeV and 0.05(0.33) fb at the 50 TeV. Typically, this cut can also reduce multi-jet QCD backgrounds, see in Table.1 and Table.2, from 0.25 fb to 0.16 fb for the CC production at the 7TeV and 1.54 fb to 0.85 fb at the 50TeV. Unfortunately, forward jet cut does not have much impact on the single top background. The final signal significance do not change much for 7 TeV, say, 4.2 compare to 4.19. And even worse for 50 TeV, say, 13.9 to 15.34. Thus in our final limit analysis we will not use it.

For a short summary and to be clear, we list all the Cut-based selections here:

- cut1: the basic pre-selection cuts in Eq.(12).
- cut2: the selection $e^-p \rightarrow \cancel{E}_T^{\text{missing}} + 0 \ell + \geq 3 \text{ jets}$, (with at least 2 tagged B – jets).
- cut3: Missing transverse energy $\cancel{E}_T^{\text{missing}} > 20 \text{ GeV}$.
- cut4: the reconstructed top quark mass window $m_t \in [148\text{GeV}, 178\text{GeV}]$.
- cut5: the reconstructed w boson mass window $m_w < 50\text{GeV}$ or $m_w > 90\text{GeV}$.
- cut6: the reconstructed z boson mass window $m_z < 55\text{GeV}$ or $m_z > 95\text{GeV}$.
- cut7: the reconstructed higgs mass window $m_h \in [100\text{GeV}, 130\text{GeV}]$.
- cut8: the forward light jet veto cut $|\eta^j| < 2.5$ for 7TeV and $|\eta^j| < 3$ for 50TeV (We do not use this for the final analysis).

After imposing all the selections(cut1-cut7, no cut8), the signal(total background) turn to be 0.137(0.93) fb and 1.29(5.8) fb for 7 and 50 TeV respectively. We see the final select efficiency for the signal(ϵ_S) respect to the sample is about 2.4(2.4)%. At the end of the Cut-based analysis we obtain a signal significance \mathcal{SS} (defined in Eq.(15)) of 4.19(15.34) correspond to the full backgrounds with 1000 fb^{-1} integrated luminosity. From Table.1 and Table.2 we also find that after applying all the selections, the most important contribution to the combinatorial background is still the single top(bakt) background which stands for 40-60 percent of the total.

7TeV@LHeC	cut1	cut2	cut3	cut4	cut5	cut6	cut7	cut8
signal0.1	5.80	0.86	0.77	0.42	0.16	0.15	0.137	0.11
bakt	1537.26	29.94	27.22	16.28	0.84	0.54	0.38	0.30
bakej	50450.7	8.66	0.89	0.24	0.04	0.01	0	0
bakvej	11190.49	21.10	20.32	3.92	1.15	0.64	0.25	0.16
bakh	63.09	10.85	9.92	1.77	0.29	0.34	0.27	0.09
bakz	71.09	9.99	9.74	1.74	0.53	0.10	0.03	0.017
Total BG	63312.63	80.54	68.09	23.96	3.05	1.63	0.93	0.57
\mathcal{R}	$< \mathcal{O}(10^{-4})$	0.011	0.011	0.017	0.05	0.094	0.147	0.197
\mathcal{P}	$< \mathcal{O}(10^{-4})$	0.011	0.011	0.017	0.05	0.086	0.128	0.164
\mathcal{SS}	$\sim \mathcal{O}(0.7)$	3.0	2.94	2.69	2.8	3.6	4.19	4.2

Table 1: Expected cross sections in unit of fb after different combinations of cuts for signal ($\kappa_{\text{tuh}} = 0.1$) and backgrounds at the LHeC. \mathcal{SS} is evaluated with 1000 fb^{-1} integrated luminosity. The LHeC colliding energy is the 7 TeV proton with a 60 GeV electron beam. Here the B-tagging efficiency is $\epsilon_b = 0.6$. The light, charm jets mis-identification rates are $\epsilon_c = 0.1$ and $\epsilon_{\text{light}} = 0.01$.

50TeV@LHeC	cut1	cut2	cut3	cut4	cut5	cut6	cut7	cut8
signal0.1	52.80	7.81	7.169	3.93	1.50	1.43	1.29	0.94
bakt	13980.68	278.20	258.66	157.68	7.37	4.67	3.25	2.39
bakej	244578.69	45.98	7.39	1.66	0.34	0.15	0.05	0
bakvej	50164.90	121.02	117.24	22.02	5.44	3.18	1.54	0.85
bakh	234.09	41.92	38.82	5.74	1.56	1.07	0.86	0.33
bakz	297.50	44.45	43.64	6.14	1.81	0.34	0.10	0.05
Total BG	309255.86	531.58	465.75	193.25	16.52	9.40	5.80	3.63
\mathcal{R}	$< \mathcal{O}(10^{-4})$	0.015	0.015	0.020	0.091	0.152	0.223	0.260
\mathcal{P}	$< \mathcal{O}(10^{-4})$	0.015	0.015	0.020	0.083	0.132	0.182	0.207
\mathcal{SS}	$\sim \mathcal{O}(3)$	10.63	10.42	8.85	11.18	13.74	15.34	13.9

Table 2: Expected cross sections in unit of fb after different combinations of cuts for signal ($\kappa_{\text{tuh}} = 0.1$) and backgrounds at the LHeC. \mathcal{SS} is evaluated with 1000 fb^{-1} integrated luminosity. The LHeC colliding energy is the 50 TeV proton with a 60 GeV electron beam. Here the B-tagging efficiency is $\epsilon_b = 0.6$. The light, charm jets mis-identification rates are $\epsilon_c = 0.1$ and $\epsilon_{\text{light}} = 0.01$.

One way to improve the signal significance is of course simply to impose more critical cut on the rejection of the reconstructed w mass. Since this is the most efficient way to reduce the bakt background. However it is not strange such a cut would reduce the signal events passing the selection as well. One of the other way might be the enhancement of the B-tagging efficiency together with the reduction of the jet mis-identification rates. In Table.3 and Table.4 we quantify the impact of light and charm jet mis-identification rates and the B-tagging efficiencies on the signal significance. This is also one part of updated results in the present study compare to our previous work in Ref.[57]. In the tables, σ_S refers to the signal cross section in the unit of fb, or number of signal events correspond to 1 fb^{-1} integrated luminosity. σ_B refers to the total contributions include both irreducible and reducible background components. For the B-tagging efficiency we choose ϵ_b equal 0.6, 0.7 and 0.8 accordingly. The signal events change from 0.14(1.29) to 0.19(1.75) and finally 0.24(2.29) fb respectively, lead 35.7(35.7)% and 26.3(30.9)% enhancement. Since the raise of B-tagging efficiency would improve the reconstruction of Higgs boson and therefore be advantageous to enhance our signal. However we should notice that the B-tagging efficiency would increase the background events as well especially the bakh background. Nevertheless, for the same C-jet fake B-jet rate (ϵ_c) of 0.1 and light jet fake B-jet rate (ϵ_{light}) of 0.01, the signal significance change from 4.19(15.34) to 5.05(18.79) and finally 6.01(22.3), correspondingly, for the choice of 1000 fb^{-1} integrated luminosity. For the decreased value of ϵ_c (0.1, 0.5 and 0.01) and ϵ_{light} (0.01 and 0.001), the background events can reduce obviously as shown in Table.3 and Table.4. These fake rate would have little impact on the signal events. Finally we can get the best signal significance of 8.37(33.75) with $\epsilon_b = 0.8$, $\epsilon_c = 0.01$ and $\epsilon_{\text{light}} = 0.001$ with the same value of the input parameters and kinematic cuts.

2.4.2 Optimized variables and TMVA framework Analysis

Now we turn to discuss Multivariate Analysis(MVA) based method. We need information the more the better in order to set limits on the cross section of the process(or the anomalous tqh couplings) being searched for. This can be obtained from counting the number

ϵ_b	ϵ_c	ϵ_{light}	σ_S	σ_B	$\mathcal{SS}[\mathcal{L} = 1000 fb^{-1}]$
60%	10%	1%	0.14	0.93	4.19
		0.1%	0.14	0.53	5.30
	5%	1%	0.14	0.78	4.52
		0.1%	0.14	0.43	5.74
	1%	1%	0.14	0.67	4.82
		0.1%	0.14	0.35	6.20
70%	10%	1%	0.19	1.16	5.05
		0.1%	0.19	0.68	6.38
	5%	1%	0.19	0.99	5.41
		0.1%	0.19	0.60	6.70
	1%	1%	0.19	0.87	5.72
		0.1%	0.19	0.50	7.16
80%	10%	1%	0.24	1.34	6.01
		0.1%	0.24	0.88	7.27
	5%	1%	0.24	1.18	6.33
		0.1%	0.24	0.71	7.91
	1%	1%	0.24	1.04	6.68
		0.1%	0.24	0.61	8.37

Table 3: Table to quantify the impact of light (ϵ_{light}), charm (ϵ_c) jet mis-identification rates and B-tagging efficiencies (ϵ_b) on our signal ($\kappa_{\text{tuh}} = 0.1$) and total backgrounds at the LHeC. The cross sections are in unit of fb. \mathcal{SS} is evaluated with 1000 fb^{-1} integrated luminosity. The LHeC colliding energy is the 7 TeV proton with a 60 GeV electron beam.

ϵ_b	ϵ_c	ϵ_{light}	σ_S	σ_B	$\mathcal{SS}[\mathcal{L} = 1000 fb^{-1}]$
60%	10%	1%	1.29	5.80	15.34
		0.1%	1.28	3.09	19.42
	5%	1%	1.29	4.82	16.53
		0.1%	1.28	2.03	22.30
	1%	1%	1.29	4.03	17.71
		0.1%	1.28	1.42	24.68
70%	10%	1%	1.74	6.84	18.79
		0.1%	1.75	3.56	24.05
	5%	1%	1.74	5.50	20.46
		0.1%	1.75	2.64	26.43
	1%	1%	1.74	4.86	21.41
		0.1%	1.75	1.82	29.32
80%	10%	1%	2.24	7.87	22.30
		0.1%	2.29	4.33	28.14
	5%	1%	2.24	6.38	24.15
		0.1%	2.29	3.30	30.62
	1%	1%	2.24	5.35	25.73
		0.1%	2.29	2.31	33.75

Table 4: Table to quantify the impact of light (ϵ_{light}), charm (ϵ_c) jet mis-identification rates and B-tagging efficiencies (ϵ_b) on our signal ($\kappa_{\text{tuh}} = 0.1$) and total backgrounds at the LHeC. The cross sections are in unit of fb. \mathcal{SS} is evaluated with 1000 fb^{-1} integrated luminosity. The LHeC colliding energy is the 50 TeV proton with a 60 GeV electron beam.

of predicted signal and background events selected by the analysis and from their relative shape. It will be useful to find a final “discriminate distribution” which shows the largest discrimination between signal and background events. Such a distribution can either be a kinematic variable, or a new distribution constructed for this task. MVA is such a method that designed to construct such a variable with a high discriminating power by exploiting predefined multiple variables. In order to perform a MVA, we use the Toolkit for Multivariate Analysis(TMVA) [69] package which provides a ROOT-integrated environment for the processing, parallel evaluation and application of multivariate classification technique. Typically, the Boosted Decision Trees(BDT) technique is chosen in our analysis.

To perform TMVA, technically, the most important but challenge thing is to define suitable variables. Choices of suitable variables depend not only on signal and background characteristics but also on suitable pre-selection. This pre-selection could be some cuts, user defined but not critical, imposed after Monte Carlo event sample. In our case, in contrast to the full critical selections in the Cut-based analysis, we choose, i.e., the cut to reject of w mass window. Though the motivation is to separate the signal and background in advance as much as possible, we should find some balance between the potential of separating and statistical uncertainty before the final decision of the pre-selection.

Depending on our signal and background topological characteristics, we define a set of totally 44 kinematic variables for BDT training, rank variables based on their gini index contributions or how often they were used as tree splitters. These variables include the jet number(N_{jet}), the B-jet number(N_{Bjet}), the transverse momentum of the jets ($p_{\text{T}}^{\text{B}_1}$, $p_{\text{T}}^{\text{B}_2}$, $p_{\text{T}}^{\text{J}_1}$) where B_1 , B_2 and J_1 are the leading B-jet, subleading B-jet and light jet; the rapidity of the jets (η^{B_1} , η^{B_2} , η^{J_1}); the azimuthal angle of the jets (Φ^{B_1} , Φ^{B_2} , Φ^{J_1}) in the range $[0, 2\pi]$; the invariant mass of the reconstructed resonances m_{Higgs} , m_{z} , m_{w} , m_{top} , the transverse momenta of the reconstructed resonances $p_{\text{T}}^{\text{Higgs}}$, p_{T}^{z} , p_{T}^{w} , $p_{\text{T}}^{\text{top}}$; the rapidity of the heavy resonances η^{Higgs} , η^{z} , η^{w} , η^{top} ; the azimuthal angle of the heavy resonances Φ^{Higgs} , Φ^{z} , Φ^{w} , Φ^{top} ; the difference in azimuthal angle between ($\Delta\Phi^{\text{B}_1\text{B}_2}$, $\Delta\Phi^{\text{B}_1\text{J}_1}$, $\Delta\Phi^{\text{B}_2\text{J}_1}$) and the Higgs jet system($\Delta\Phi^{\text{hJ}_1}$); the separation in the $\Phi - \eta$ plane between jets ($\Delta\text{R}^{\text{B}_1\text{B}_2}$, $\Delta\text{R}^{\text{B}_1\text{J}_1}$, $\Delta\text{R}^{\text{B}_2\text{J}_1}$) and the Higgs jet system($\Delta\text{R}^{\text{hJ}_1}$); the difference in $|\eta|$ between jets

$(\Delta\eta^{B_1B_2}, \Delta\eta^{B_1J_1}, \Delta\eta^{B_2J_1})$ and the Higgs jet system($\Delta\eta^{hJ_1}$); the missing transverse(MET) energy $\cancel{E}_T^{\text{missing}}$; and the vector sum of the Higgs MET system, the top MET system, the z MET system and the w MET system. Full list of 44 variables pertaining to both background and signal was narrowed down to 32 variables using TMVA in our analysis. Indeed, we test and compare and find that 9 within 32 of them are the most powerful variables which are: $N_{\text{Bjet}}, \Delta R^{B_1J_1}, \Delta\Phi^{B_1J_1}, \Delta\Phi^{B_1B_2}, \Delta R^{B_1B_2}, p_T^{J_1}, \Delta\eta^{hJ_1}, m_w$ and m_h .

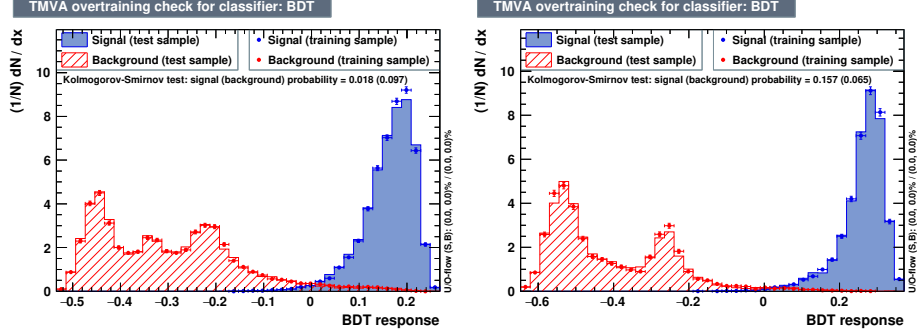


Figure 6: Normalized signal and background distributions against BDT response for $\kappa_{\text{tuh}} = 0.1$. Left panel for 7TeV and right panel for 50TeV.

Both our signal and backgrounds are trained by the BDT algorithm and another set of event samples are used to test the BDT output. We should always be alert not to overtrain signal and background. The universally accepted Kolmogorov-Smirnov (KS) test can reveal if our choice of variables needs to be changed. The test sample is not overtrained if the KS probability lies in the range (0.1,0.9)[70]. For most cases, a critical value of the KS probability greater than 0.01[71] implies that the samples are not overtrained. In our subsequent study we ensure that overtraining is not an issue over our parameter space. In Fig.6 we present the output distributions for the signal and background sample for a given classifier(in this case BDT, i.e. Boosted Decision Trees). The signal in the blue area is for $\kappa_{\text{tuh}} = 0.1$. The red area refers to the total backgrounds. Notice the plots are all normalized to equal area respectively, so more blue area(signal) outside the red area(background) means the variable is more discriminative against background. For the intent of our analysis, the lump in the area larger than zero should be worked around. The BDT output is indeed such a constructed variable with a high discriminating power

by exploiting predefined multiple variables. The normalized distributions of the signal and background as a function of these multiple variables can be output automatically from the TMVA framework. There we expect areas as widely separated as possible, in order to make a good signal background discrimination.

7TeV@LHeC	$C_{\text{BDT}} > 0.09$	$C_{\text{BDT}} > 0.11$	$C_{\text{BDT}} > 0.13$	$C_{\text{BDT}} > 0.15$	$C_{\text{BDT}} > 0.17$
signal0.1	0.145937	0.137367	0.125014	0.107273	0.0841252
total BG	0.916963	0.7132	0.520381	0.38794	0.24486
\mathcal{R}	0.159	0.193	0.240	0.277	0.344
\mathcal{P}	0.137	0.162	0.194	0.217	0.256
\mathcal{SS}	4.476	4.710	4.921	4.821	4.638

Table 5: Expected signal ($\kappa_{\text{tuh}} = 0.1$) and background cross sections after BDT cut. \mathcal{SS} is evaluated with 1000 fb^{-1} integrated luminosity at the LHeC. The colliding energy is the 7 TeV proton with a 60 GeV electron beam. Here the B-tagging efficiency ($\epsilon_b = 0.6$) and non-Bjet mis-tagging rates ($\epsilon_c = 0.1$ and $\epsilon_{\text{light}} = 0.01$) are taken into accounts.

In Table.5 and Table.6 we present the expected signal($\kappa_{\text{tuh}} = 0.1$) and background cross sections after a set of different BDT cuts(C_{BDT}). The background(“total BG”) include all different components. Here the B-tagging efficiency($\epsilon_b = 0.6$) and non-Bjet mis-tagging rates ($\epsilon_c = 0.1$ and $\epsilon_{\text{light}} = 0.01$) are taken into accounts. The value of \mathcal{R} , \mathcal{P} and \mathcal{SS} are evaluated with 1000 fb^{-1} integrated luminosity at the LHeC. The colliding energy is the 7(50) TeV proton with a 60 GeV electron beam. These parameters are the same as in the Cut-based analysis. We find for $C_{\text{BDT}} > 0.13(0.22)$, we have the signal significance equal 4.921(16.934). Compare to Cut-based results, we have the largest \mathcal{SS} equal 4.19(15.34). As expected, we find the MVA based method can help us to achieve better signal significance with respect to the Cut-based analysis.

50TeV@LHeC	$C_{\text{BDT}} > 0.18$	$C_{\text{BDT}} > 0.20$	$C_{\text{BDT}} > 0.22$	$C_{\text{BDT}} > 0.24$	$C_{\text{BDT}} > 0.26$
signal0.1	0.723866	0.694838	0.65193	0.585753	0.479036
total BG	1.51567	1.1335	0.830125	0.655706	0.425236
\mathcal{R}	0.478	0.613	0.785	0.893	1.127
\mathcal{P}	0.323	0.380	0.440	0.472	0.530
\mathcal{SS}	15.296	16.250	16.934	16.624	15.930

Table 6: Expected signal ($\kappa_{\text{tuh}} = 0.1$) and background cross sections after BDT cut. \mathcal{SS} is evaluated with 1000 fb^{-1} integrated luminosity at the LHeC. The colliding energy is the 50TeV proton with a 60 GeV electron beam. Here the B-tagging efficiency ($\epsilon_b = 0.6$) and non-Bjet mis-tagging rates ($\epsilon_c = 0.1$ and $\epsilon_{\text{light}} = 0.01$) are taken into accounts.

2.4.3 Discovery Potential

We follow refs [72][73] exactly to obtain the sensitivity limits. A chi-square (χ^2) analysis is performed with the definition

$$\chi^2 = \left(\frac{\sigma_{\text{tot}} - \sigma_B}{\sigma_B \delta} \right)^2 \quad (18)$$

where σ_{tot} is the cross section containing new physics effects and $\delta = \frac{1}{\sqrt{N}}$ is the statistical error with $N = \sigma_B \times \mathcal{L} \times \epsilon$. The parameter sensitivity limits on anomalous tqH coupling as a function of the integrated luminosity can then be achieved.

Fig.7 shows the upper limit of $\text{Br}(t \rightarrow uh)$ at 99.9, 95 and 68% C.L. as a function of the integrated luminosity at the LHeC. The red, blue and black curves represent the one, two and five standard deviation bands around the expectation. The limit from Cut-based analysis is present in the first two panels and is compared with the TMVA framework analysis which is shown in the second two panels. For the 7 TeV LHeC, we see the analysis is able to probe $\text{Br}(t \rightarrow uh)$ down to 0.113% at 1σ level, corresponding to an upper limit on the κ_{tuh} coupling of 0.047, with 1000 fb^{-1} integrated luminosity with our Cut-based analysis. This is a little worse than our TMVA framework analysis with which we can probe $\text{Br}(t \rightarrow uh)$ down to 0.093% with the same value of the integrated luminosity.

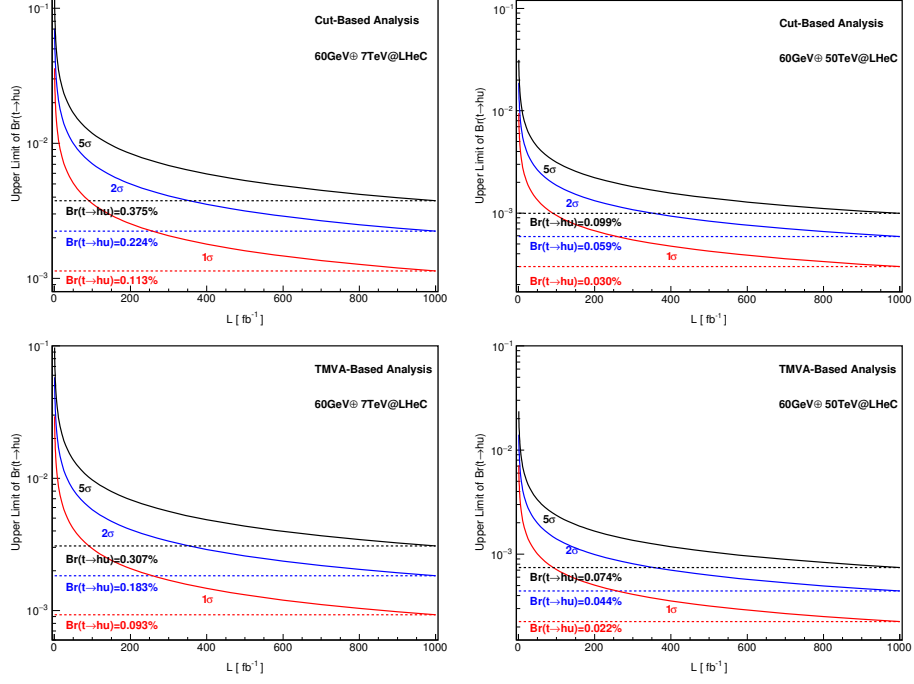


Figure 7: The upper limit on $\text{Br}(t \rightarrow uh)$ at 99.9, 95, 68% C.L. as a function of the integrated luminosity at the 7(50) TeV LHeC with 60 GeV electron beam. The red, blue and black curves present 1σ , 2σ and 5σ systematics. Both limits from the Cut-based method [first two panels] and the TMVA based method [second two panels] are performed.

And this is corresponding to an upper limit on the κ_{tuh} coupling of 0.042. All these are not as good as 50 TeV high energy LHeC where we can probe $\text{Br}(t \rightarrow uh)$ down to 0.03(0.022)% with the same value of the integrated luminosity. And this is corresponding to an upper limit on the κ_{tuh} coupling of 0.024(0.02) correspond to the Cut-based(TMVA-based) methods. We can see the 50 TeV high energy LHeC would improve the search sensitivities than the 7TeV one. We remind here the B-tagging efficiency is $\epsilon_b = 0.6$ and the jet mis-identification rates are the default value of $\epsilon_c = 0.1$ and $\epsilon_{\text{light}} = 0.01$ respectively.

Finally, a detailed comparison between our study and the critical limits obtained by the experiments and by the phenomenological studies are shown in Table.7 and Table.8. In Table.7 we present the integrated luminosity (\mathcal{L}) needed to get the upper bounds on the $\text{Br}(t \rightarrow qh)$ at 95% C.L. obtained from the experiments. While in Table.8 we present the \mathcal{L} needed to get the upper bounds on the $\text{Br}(t \rightarrow qh)$ at 95% C.L. (or 3σ in [76]) obtained from the phenomenological studies. We thus have an overview of the searching potential of tqh anomalous couplings at the LHeC collider(s) compare to studies at the LHC or linear colliders.

3 CONCLUSION

In this paper we have investigated an updated analysis on searches for the anomalous flavor changing neutral current(FCNC) Yukawa interactions between the top quark, the Higgs boson, and either an up or charm quark(tqh, $q = u, c$). We probe the observability of the FCNC top-Higgs couplings through the process $e^-p \rightarrow \nu_e \bar{t} \rightarrow \nu_e h \bar{q}$ at the Large Hadron Electron Collider(LHeC) where the Higgs boson decays to a $b\bar{b}$ pair. We perform the results from both the Cut-based method and the Multivariate Analysis(MVA) based method. With suitable kinematic selections we apply and optimized variables we choose, we can get the signal significance(\mathcal{SS}) of 4.19(15.34) for 7(50) TeV LHeC from the cut

Channels and Limits	Method	7TeV@LHeC		50TeV@LHeC	
		$\mathcal{L}[\text{fb}^{-1}]_{2\sigma}$	$\mathcal{L}[\text{fb}^{-1}]_{1\sigma}$	$\mathcal{L}[\text{fb}^{-1}]_{2\sigma}$	$\mathcal{L}[\text{fb}^{-1}]_{1\sigma}$
$t\bar{t} \rightarrow \text{Wbqh} \rightarrow \ell\nu b\gamma\gamma q$ CMS, 19.5 fb ⁻¹ @8TeV Br($t \rightarrow \text{uh}$) < 0.45% [41]	Cut	246.7	63.5.5	17.3	4.5
	TMVA	165.6	42.6	9.7	2.5
$t\bar{t} \rightarrow \text{Wbqh} \rightarrow \ell\nu b\gamma\gamma q$ ATLAS, 4.7(20.3)fb ⁻¹ @7(8)TeV Br($t \rightarrow \text{qh}$) < 0.79%[42][43]	Cut	80.1	20.6	5.6	1.4
	TMVA	53.7	13.8	3.2	0.8
$D^0 - \bar{D}^0$ mixing data Br($t \rightarrow \text{qh}$) < 0.5%[44]	Cut	199.9	51.5	14.0	3.6
	TMVA	134.1	34.5	7.9	2.0
$Z \rightarrow c\bar{c}$ and EW observables Br($t \rightarrow \text{qh}$) < 0.21%[74]	Cut	1.13 _{pb} ⁻¹	291.7	79.3	20.4
	TMVA	0.76 _{pb} ⁻¹	195.7	44.6	11.5

Table 7: The integrated luminosity (\mathcal{L}) needed to get the upper bounds on the Br($t \rightarrow \text{qh}$) at 95% C.L. obtained from the experiments. Both the Cut(TMVA) based results and 1 σ (2 σ) limits are presented.

Channels and Limits	Method	7TeV@LHeC		50TeV@LHeC	
		$\mathcal{L}[\text{fb}^{-1}]_{2\sigma}$	$\mathcal{L}[\text{fb}^{-1}]_{1\sigma}$	$\mathcal{L}[\text{fb}^{-1}]_{2\sigma}$	$\mathcal{L}[\text{fb}^{-1}]_{1\sigma}$
$t\bar{t} \rightarrow Wbqh \rightarrow \ell\nu b\gamma\gamma q$ LHC, 3000 fb ⁻¹ @14TeV Br(t \rightarrow uh) < 0.23% [46]	Cut	0.94 _{pb⁻¹}	243.2	66.1	17.0
	TMVA	0.63 _{pb⁻¹}	163.2	37.2	9.6
$th \rightarrow \ell\nu b\tau^+\tau^-$ LHC, 100 fb ⁻¹ @13TeV Br(t \rightarrow uh) < 0.15%[48]	Cut	2.22 _{pb⁻¹}	0.57 _{pb⁻¹}	155.5	40.0
	TMVA	1.49 _{pb⁻¹}	0.38 _{pb⁻¹}	87.4	22.5
$th \rightarrow \ell\nu b\ell^+\ell^-X$ LHC, 100 fb ⁻¹ @13TeV Br(t \rightarrow uh) < 0.22%[48]	Cut	1.03 _{pb⁻¹}	0.27 _{pb⁻¹}	72.3	18.6
	TMVA	0.69 _{pb⁻¹}	0.18 _{pb⁻¹}	40.6	10.5
$th \rightarrow jjbb\bar{b}$ LHC, 100 fb ⁻¹ @13TeV Br(t \rightarrow uh) < 0.36%[48]	Cut	385.5	99.3	27.0	7.0
	TMVA	258.7	66.6	15.2	3.9
$t\bar{t} \rightarrow tqh \rightarrow \ell\nu b\bar{b}bq$ ILC, 3000 fb ⁻¹ @500GeV Br(t \rightarrow qh) < 0.112%[75]	Cut	3.98 _{pb⁻¹}	1.03 _{pb⁻¹}	278.8	71.8
	TMVA	2.67 _{pb⁻¹}	0.69 _{pb⁻¹}	156.7	40.3
$Wt \rightarrow Whq \rightarrow \ell\nu b\gamma\gamma q$ LHC, 3000 fb ⁻¹ @14TeV 3 σ , Br(t \rightarrow qh) < 0.24%[76]	Cut	867.5	223.3	60.7	15.6
	TMVA	582.1	149.9	34.1	8.8

Table 8: The integrated luminosity (\mathcal{L}) needed to get the upper bounds on the Br(t \rightarrow qh) at 95% C.L. (or 3 σ) obtained from some other phenomenological studies. Both the Cut(TMVA) based results and 1 σ (2 σ) limits are presented.

based method. The \mathcal{SS} can be improved to 4.921(16.934) with the identical conventions and parameter sets if the MVA framework is applied. Our results show that, at a 7 TeV LHeC with a 60 GeV electron beam and 1000 fb^{-1} luminosity, the expected limit on $\text{Br}(t \rightarrow qh)$ can be probed down to 0.113(0.093)% with the Cut-based(MVA based) analysis at the 95% confidence level. For the 50 TeV LHeC, these limits can be probed down to 0.03(0.022)%. Here the B-tagging efficiencies, charm and light jet mis-identification rates are chosen to be 0.6, 0.1, and 0.01 respectively. We also quantify the impact of light, charm jet mis-identification rates and B-tagging efficiencies on the discovery potential. For instance, for $\epsilon_b = 0.6$, $\epsilon_c = 0.01$ and $\epsilon_{\text{light}} = 0.001$, the signal significance can be improved to be larger than $\mathcal{SS} \sim 20$ at 50 TeV LHeC. The limits are expected to improve if the MVA framework is applied. We also present a detailed comparison between our study and the critical limits obtained by the experiments and by some other phenomenological studies. Our results are better than the most stringent constraint of $\text{Br}(t \rightarrow qh) < 0.56\%$ [41] and $\text{Br}(t \rightarrow qh) < 0.79\%$ [42][43] at 95% C.L. from the CMS and ATLAS Collaborations. Furthermore, our results are comparable with those of other phenomenological studies. We thus give a overview of searching potential on the anomalous top-Higgs couplings at the LHeC.

Acknowledgments

Hao Sun acknowledges Fawzi Boudjema for his warm hospitality at LAPTh, thanks Shankha Banerjee for his help with computing facilities used in this work, thanks Antje Putze and Caroff Sami for useful discussions. Project supported by the National Natural Science Foundation of China (Grant No. 11205070), by the Fundamental Research Funds for the Central Universities (Grant No. DUT15LK22) and by China Scholarship Council (Grant CSC No. 201406065026).

References

- [1] G. Aad, et al., [ATLAS Collaboration], *Observation of a new particle in the search for the Standard Model Higgs boson with the ATLAS detector at the LHC*, Phys. Lett. B 716 (2012) 1-29, [arXiv:1207.7214].
- [2] S. Chatrchyan, et al., [CMS Collaboration], *Observation of a new boson at a mass of 125 GeV with the CMS experiment at the LHC*, Phys. Lett. B 716 (2012) 30, [arXiv:1207.7235].
- [3] S. Glashow, J. Iliopoulos, and L. Maiani, *Weak Interactions with Lepton-Hadron Symmetry*, Phys. Rev. D 2 (1970) 1285.
- [4] Aguilar-Saavedra, *Top flavor-changing neutral interactions: Theoretical expectations and experimental detection*, Acta Phys. Polon. B 35 (2004) 2695, [hep-ph/0409342].
- [5] C. S. Li, R. J. Oakes, and J. M. Yang, *Rare decay of the top quark in the minimal supersymmetric model*, Phys. Rev. D 49 (1994) 293. Erratum-ibid.D 56 (1997) 3156.
- [6] G. M. de Divitiis, R. Petronzio, and L. Silvestrini, *Flavour-changing top decays in supersymmetric extensions of the standard model*, Nucl. Phys. B 504 (1997) 45, [hep-ph/9704244].
- [7] J. L. Lopez, D. V. Nanopoulos, and R. Rangarajan, *New supersymmetric contributions to $t \rightarrow cV$* , Phys. Rev. D 56 (1997) 3100, [hep-ph/9702350].
- [8] Jin Min Yang, Bing-Lin Young, and X. Zhang, *Flavor-changing Top Quark Decays In R-Parity Violating SUSY*, Phys. Rev. D 58 (1998) 055001, [arXiv:hep-ph/9705341].
- [9] J. Guasch and J. Sola, *FCNC top quark decays: A door to SUSY physics in high luminosity colliders?*, Nucl. Phys. B 562 (1999) 3, [hep-ph/9906268].
- [10] G. Eilam, A. Gemintern, T. Han, J.M. Yang, and X. Zhang, *Top-quark rare decay $t \rightarrow ch$ in R-parity-violating SUSY*, Phys. Lett. B 510 (2001) 227-235, [arXiv:hep-ph/0102037].

- [11] D. Delepine and S. Khalil, *Top flavour violating decays in general supersymmetric models*, Phys. Lett. B 599 (2004) 62, [hep-ph/0406264].
- [12] J. J. Liu, C. S. Li, L. L. Yang, and L. G. Jin, *$t \rightarrow cV$ via SUSY FCNC couplings in the unconstrained MSSM*, Phys. Lett. B 599 (2004) 92, [hep-ph/0406155].
- [13] J.J.Cao, G.Eilam, M.Frank, K.Hikasa, G.L.Liu, I.Turan, and J. M. Yang, *SUSY-induced FCNC top-quark processes at the Large Hadron Collider*, Phys. Rev. D 75 (2007) 075021, [arXiv:hep-ph/0702264].
- [14] David Lopez-Val, Jaume Guasch, and Joan Sola, *Single top-quark production by strong and electroweak supersymmetric flavor-changing interactions at the LHC*, JHEP 0712 (2007) 054, [arXiv:0710.0587].
- [15] Junjie Cao, Zhaoxia Heng, Lei Wu, and Jin Min Yang, *R-parity violating effects in top quark FCNC productions at LHC*, Phys. Rev. D 79 (2009) 054003, [arXiv:0812.1698].
- [16] A. Dedes, M. Paraskevas, J. Rosiek, K. Suxho, and K. Tamvakis, *Rare Top-quark Decays to Higgs boson in MSSM*, JHEP 1411 (2014) 137, [arXiv:1409.6546].
- [17] Junjie Cao, Chengcheng Han, Lei Wu, Jin Min Yang, and Mengchao Zhang, *SUSY induced top quark FCNC decay $t \rightarrow cH$ after Run I of LHC*, Eur. Phys. J. C 74 (2014) 9, 3058, [arXiv:1404.1241].
- [18] Tie-Jun Gao, Tai-Fu Feng, Fei Sun, Hai-Bin Zhang, and Shu-Min Zhao, *Top quark decay to a 125GeV Higgs in BLMSSM*, Chin. Phys. C 39 (2015) 7, 073101, [arXiv:1404.3289].
- [19] J.L. Diaz-Cruz, Hong-Jian He, and C.-P. Yuan, *Soft Supersymmetry Breaking, Scalar Top-Charm Mixing and Higgs Signatures*, Phys. Lett. B 530 (2002) 179, [hep-ph/0103178].

- [20] B. Grzadkowski, J. F. Gunion, and P. Krawczyk, *Neutral current flavor changing decays for the Z boson and the top quark in two Higgs doublet models*, Phys. Lett. B 268 (1991) 106.
- [21] G. Eilam, J.L. Hewett, and A. Soni, *Rare decays of the top quark in the standard and two Higgs doublet models*, Phys. Rev. D 44 (1991) 1473-1484, Erratum-ibid. D 59 (1999) 039901.
- [22] D. Atwood, L. Reina, and A. Soni, *Phenomenology of two Higgs doublet models with flavor changing neutral currents*, Phys. Rev. D 55 (1997) 3156, [hep-ph/9609279].
- [23] S. Bejar, J. Guasch, and J. Sola, *Loop induced flavor changing neutral decays of the top quark in a general two-Higgs-doublet model*, Nucl. Phys. B 600 (2001) 21, [hep-ph/0011091].
- [24] Santi Bejar, Jaume Guasch, and Joan Sola, *Higgs Boson Flavor-Changing Neutral Decays into Top Quark in a General Two-Higgs-Doublet Model*, Nucl. Phys. B 675 (2003) 270-288, [arXiv:hep-ph/0307144].
- [25] I. Baum, G. Eilam, and S. Bar-Shalom, *Scalar FCNC and rare top decays in a two Higgs doublet model for the top*, Phys. Rev. D 77 (2008) 113008, [hep-ph/0802.2622].
- [26] Chung Kao, Hai-Yang Cheng, Wei-Shu Hou, and Joshua Sayre, *Top Decays with Flavor Changing Neutral Higgs Interactions at the LHC*, Phys.Lett. B 716 (2012) 225-230, [arXiv:1112.1707].
- [27] K.-F. Chen, W.-S. Hou, C. Kao, and M. Kohda, *When the Higgs meets the Top: Search for $t \rightarrow ch^0$ at the LHC*, Phys. Lett. B 725 (2013) 378, [arXiv:1304.8037].
- [28] D. Atwood, S. K. Gupta, and A. Soni, *Constraining the flavor changing Higgs couplings to the top-quark at the LHC*, JHEP 1410 (2014) 57, [arXiv:1305.2427].

- [29] Kai-Feng Chen, Wei-Shu Hou, Chung Kao, and Masaya Kohda, *When the Higgs meets the Top: Search for $t \rightarrow ch^0$ at the LHC*, Phys. Lett. B 725 (2013) 378-381, [arXiv:1304.8037].
- [30] Hong-Jian He, Shinya Kanemura, and C.-P. Yuan, *Determining the Chirality of Yukawa Couplings via Single Charged Higgs Boson Production in Polarized Photon Collision*, Phys. Rev. Lett. 89 (2002) 101803, [hep-ph/0203090].
- [31] Hong-Jian He, Shinya Kanemura, and C.-P. Yuan, *Single Charged Higgs Boson Production in Polarized Photon Collision and the Probe of New Physics*, Phys. Rev. D 68 (2003) 075010, [hep-ph/0209376].
- [32] Aleksandr Azatov, Manuel Toharia, and Lijun Zhu, *Higgs Mediated FCNC's in Warped Extra Dimensions*, Phys. Rev. D 80 (2009) 035016, [arXiv:0906.1990].
- [33] S. Casagrande, F. Goertz, U. Haisch, M. Neubert, and T. Pfoh, *The Custodial Randall-Sundrum Model: From Precision Tests to Higgs Physics*, JHEP 1009 (2010) 014, [arXiv:1005.4315].
- [34] R. Gaitan, O. Miranda, and L. Cabral-Rosetti, *Rare top quark and Higgs boson decays in Alternative Left-Right Symmetric Models*, Phys. Rev. D 72 (2005) 034018, [arXiv:hep-ph/0410268]; *Rare top quark decays in extended models*, AIP Conf. Proc. 857, 179 (2006), [arXiv:hep-ph/0604170].
- [35] Bingfang Yang, Ning Liu, and Jinzhong Han, *Top Quark FCNC Decay to 125GeV Higgs boson in the Littlest Higgs Model with T -parity*, Phys. Rev. D 89 (2014) 3, 034020, [arXiv:1308.4852].
- [36] F. del Aguila, J. A. Aguilar-Saavedra, and R. Miquel, *Constraints on top couplings in models with exotic quarks*, Phys. Rev. Lett. 82 (1999) 1628.
- [37] J. A. Aguilar-Saavedra and B. M. Nobre, *Rare top decays $t \rightarrow c\gamma$, $t \rightarrow cg$ and CKM unitarity*, Phys. Lett. B 553 (2003) 251, [hep-ph/0210360].

- [38] J. Aguilar-Saavedra, *Effects of mixing with quark singlets*, Phys. Rev.D 67 (2003) 035003, [hep-ph/0210112]. Erratum-ibid. D 69 (2004) 099901.
- [39] C. S. Li, R. J. Oakes, and T. C. Yuan, *QCD corrections to $t \rightarrow W^+b$* , Phys. Rev. D 43 (1991) 3759-3762.
- [40] Wei-Shu Hou, *Tree level $t \rightarrow ch$ or $h \rightarrow t\bar{c}$ decays*, Phys. Lett. B 296 (1992) 179-184.
- [41] [CMS Collaboration], *Searches for heavy Higgs bosons in two-Higgs-doublet models and for $t \rightarrow ch$ decay using multilepton and diphoton final states in pp collisions at 8 TeV*, Phys. Rev. D 90 (2014) 112013, CMS-HIG-13-025, CERN-PH-EP-2014-239, [arXiv:1410.2751]. [CMS Collaboration], *Combined multilepton and diphoton limit on $t \rightarrow cH$* , CMS-PAS-HIG-13-034 (2014).
- [42] G. Aad et al., [ATLAS Collaboration], *Search for top quark decays $t \rightarrow qH$ with $H \rightarrow \gamma\gamma$ using the ATLAS detector*, JHEP 06 (2014) 008, CERN-PH-EP-2014-036 (2014), [arXiv:1403.6293].
- [43] *Search for flavour changing neutral currents in top quark decays $t \rightarrow cH$, with $H \rightarrow \gamma\gamma$, and limit on the tcH coupling with the ATLAS detector at the LHC*, ATLAS-CONF-2013-081 (2013).
- [44] J. I. Aranda, A. Cordero-Cid, F. Ramirez-Zavaleta, J.J. Toscano, and E.S. Tututi, *Higgs mediated flavor violating top quark decays $t \rightarrow u_i H, u_i \gamma, u_i \gamma\gamma$, and the process $\gamma\gamma \rightarrow tc$ in effective theories*, Phys. Rev. D 81 (2010) 077701, [arXiv:0911.2304].
- [45] David Atwood, Sudhir Kumar Gupta, and Amarjit Soni, *Constraining the flavor changing Higgs couplings to the top-quark at the LHC*, JHEP 1410 (2014) 57, [arXiv:1305.2427].
- [46] Lei Wu, *Enhancing thj Production from Top-Higgs FCNC Couplings*, JHEP 02 (2015) 061, [arXiv:1407.6113].

- [47] K. Agashe et al., [Top Quark Working Group Collaboration], *Snowmass 2013 Top quark working group report*, arXiv:1311.2028 [hep-ph].
- [48] Admir Greljo, Jernej F. Kamenik, and Joachim Kopp, *Disentangling Flavor Violation in the Top-Higgs Sector at the LHC*, JHEP 1407 (2014) 046, [arXiv:1404.1278].
- [49] Martin Gorbahn and Ulrich Haisch, *Searching for $t \rightarrow c(u)h$ with dipole moments*, JHEP 1406 (2014) 033, [arXiv:1404.4873].
- [50] Cen Zhang and Fabio Maltoni, *Top-quark decay into Higgs boson and a light quark at next-to-leading order in QCD*, Phys. Rev. D. 88 (2013) 054005, [arXiv:1305.7386].
- [51] Yan Wang, Fa Peng Huang, Chong Sheng Li, Bo Hua Li, Ding Yu Shao, and Jian Wang, *Constraints on flavor-changing neutral-current Htq couplings from the signal of tH associated production with QCD next-to-leading order accuracy at the LHC*, Phys. Rev. D 86 (2012) 094014, [arXiv:1208.2902].
- [52] Nathaniel Craig, Jared A. Evans, Richard Gray, Michael Park, Sunil Somalwar, Scott Thomas, and Matthew Walker, *Searching for $t \rightarrow ch$ with multileptons*, Phys. Rev. D 86 (2012) 075002, [arXiv:1207.6794].
- [53] Sara Khatibi and Mojtaba Mohammadi Najafabadi, *Probing the Anomalous FCNC Interactions in Top-Higgs Final State and Charge Ratio Approach*, Phys. Rev. D 89 (2014) 054011, [arXiv:1402.3073].
- [54] Baris Altunkaynak, Wei-Shu Hou, Chung Kao, Masaya Kohda, and Brent McCoy, *Flavor Changing Heavy Higgs Interactions at the LHC*, Phys. Lett. B 751 (2015) 135-142, [arXiv:1506.00651].
- [55] Hoda Hesari, Hamzeh Khanpour, and Mojtaba Mohammadi Najafabadi, *Direct and Indirect Searches for Top-Higgs FCNC Couplings*, Phys. Rev. D 92 (2015) 11, 113012, [arXiv:1508.07579].

- [56] Hong-Jian He and C.-P. Yuan, *New Method for Detecting Charged (Pseudo-)Scalars at Colliders*, Phys. Rev. Lett. 83 (1999) 28, [hep-ph/9810367].
- [57] Wei Liu, Hao Sun, XiaoJuan Wang, and Xuan Luo, *Probing the anomalous FCNC top-Higgs Yukawa couplings at the Large Hadron Electron Collider*, Phys. Rev. D 92 (2015) 7, 074015, [arXiv:1507.03264].
- [58] A. Alloul, N. D. Christensen, C. Degrande, C. Duhr, and B. Fuks, *FeynRules 2.0 - A complete toolbox for tree-level phenomenology*, Comput. Phys. Commun. 185, 2250-2300 (2014), [arXiv:1310.1921].
- [59] C. Degrande, C. Duhr, B. Fuks, D. Grellscheid, O. Mattelaer, and T. Reiter, *UFO the universal FeynRules output*, Comput. Phys. Commun. 183, 1201-1214 (2012), [arXiv:1108.2040].
- [60] J. Alwall, R. Frederix, S. Frixione, V. Hirschi, F. Maltoni, O. Mattelaer, H.-S. Shao, T. Stelzer, P. Torrielli, and M. Zaro, *The automated computation of tree-level and next-to-leading order differential cross sections, and their matching to parton shower simulations*, JHEP 1407, 079 (2014), [arXiv:1405.0301].
- [61] T. Sjostrand, S. Mrenna, and P. Z. Skands, *PYTHIA 6.4 Physics and Manual*, JHEP 0605, 026 (2006), [hep-ph/0603175].
- [62] J. Pumplin, D. R. Stump, J. Huston, H.L. Lai, P. M. Nadolsky, and W.K. Tung, *New generation of parton distributions with uncertainties from global QCD analysis*, JHEP 0207 (2002) 012, [arXiv:hep-ph/0201195]; D. Stump, J. Huston, J. Pumplin, W.-K. Tung, H.L. Lai, S. Kuhlmann, and J.F. Owens, *Inclusive jet production, parton distributions, and the search for new physics*, JHEP 0310 (2003) 046.
- [63] M. Cacciari, G. P. Salam, and G. Soyez, *FastJet User Manual*, Eur. Phys. J. C 72, 1896 (2012), [arXiv:1111.6097].
- [64] M. Cacciari, G. P. Salam, and G. Soyez, *The Anti- $k(t)$ jet clustering algorithm*, JHEP 0804, 063 (2008), [arXiv:0802.1189].

- [65] M.Klein, *Development of the FCC-he Study*, In FCC Physics, Detector and Accelerator Workshop, Istanbul, March 2016.
- [66] Oliver Brüening, Max Klein, *The Large Hadron Electron Collider*, Mod.Phys.Lett.A, Vol.28, No.16 (2013) 1330011, LHeC-Note-2013-001 GEN, [arXiv:1305.2090].
- [67] T. Han, B. Mellado, *Higgs Boson Searches and the Higgs Coupling at the LHeC*, Phys. Rev. D 82 (2010) 016009, [arXiv:0909.2460].
- [68] J. Hernandez-Sanchez, S.P. Das, S. Moretti, Alfonso Rosado and Reyna Xoxocotzi-Aguilar, *Flavor violating signatures of lighter and heavier Higgs bosons within Two Higgs Doublet Model type III at the LHeC*, PoS DIS2015 (2015) 227, [arXiv:1503.01464].
- [69] A. Hoecker, et.al., *TMVA - Toolkit for Multivariate Data Analysis*, PoS ACAT (2007) 040, CERN-OPEN-2007-007, [arXiv:physics/0703039].
- [70] Shankha Banerjee, Manimala Mitra, and Michael Spannowsky, *Searching for a heavy Higgs boson in a Higgs-portal BL model*, Phys. Rev. D 92 (2015) 055013, [arXiv:1506.06415].
- [71] D. Ciupke, *Study of BDT training configurations with an application to the $Z/H \rightarrow \tau\tau \rightarrow ee$ analysis*, <http://www.desy.de/f/students/2012/reports/david.ciupke.pdf.gz>
- [72] M.Köksal, S. C. Inan, *Anomalous $tq\gamma$ couplings in γp collision at the LHC*, Advances in High Energy Physics, 935840(2014), [arXiv:1305.7096].
- [73] Hao Sun, *Probe Anomalous $tq\gamma$ couplings through Single Top Photoproduction at the LHC*, Nucl. Phys. B 886 (2014) 691-711, [arXiv:1402.1817].
- [74] F. Larios, R. Martinez, M.A. Perez *Constraints on top quark FCNC from electroweak precision measurements*, Phys.Rev. D72 (2005) 057504, [arXiv:hep-ph/0412222].

- [75] Hoda Hesari, Hamzeh Khanpour, Mojtaba Mohammadi Najafabadi, *Direct and Indirect Searches for Top-Higgs FCNC Couplings*, Phys.Rev. D92 (2015) 11, 113012, [arXiv:1508.07579].
- [76] Yao-Bei Liu, Zhen-Jun Xiao, *Searches for top-Higgs FCNC couplings via Whj signal with $h \rightarrow \gamma\gamma$ at the LHC*, [arXiv:1605.01179].